CHAPTER III
RESULTS AND DISCUSSION

Aluminum hydroxide hydrate ($Al(OH)_3.xH_2O$), the starting material, for these experiments, was calculated as alumina (Al_2O_3) in this thesis. Therefore, before running experiments, the starting material was calcined using the TGA to obtain the exact percentage of Al_2O_3, as indicated by the % ceramic yield. The typical Al_2O_3 content was 54.4 %, as shown in Figure 3.1. This value was used throughout the experiments.

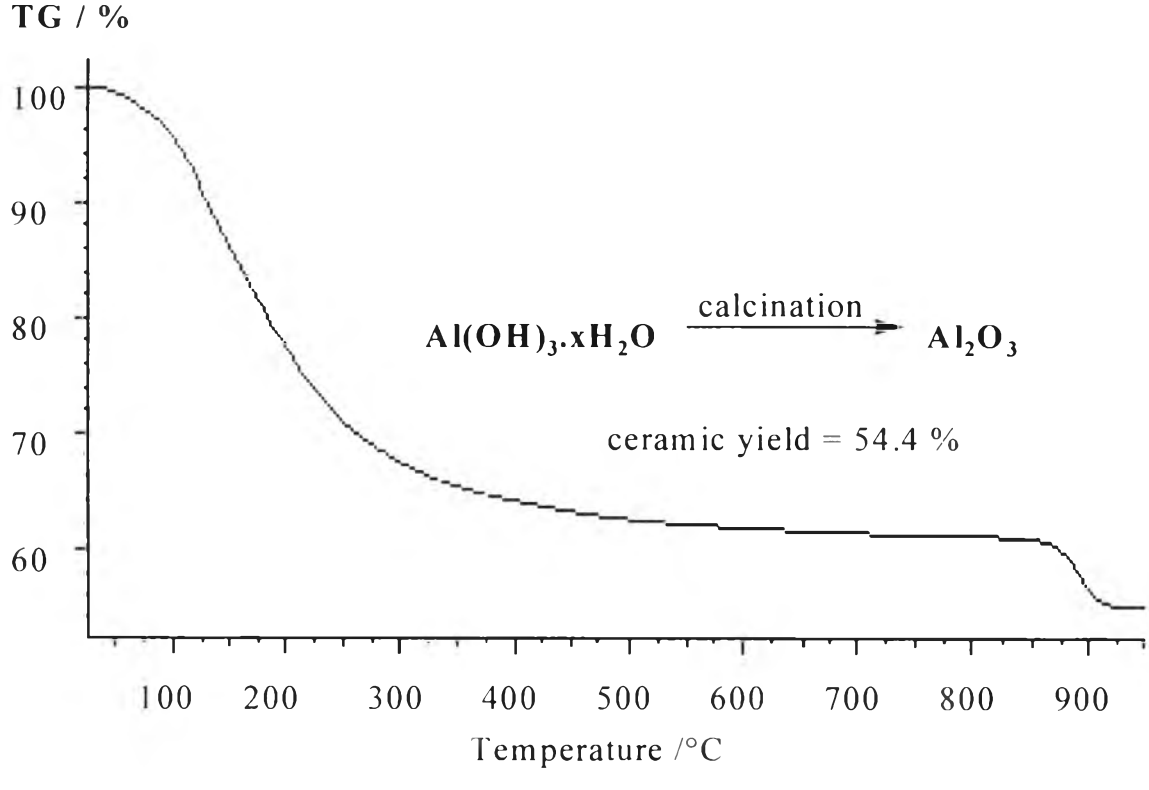

Figure 3.1 TGA Thermogram of $Al(OH)_3.xH_2O$.

3.1 Synthesis of Alumatrane Complexes

The product obtained directly from $Al(OH)_3$ and TIS was purified by precipitation with dried acetronitrile. The precipitate was soluble in both methanol and ethylene glycol, slightly soluble and swelled in other organic solvents, such as, methylene chloride, acetone, toluene and THF. This product was sensitive to the air and moisture.

3.1.1 Variation of $Al(OH)_3$: TIS Mole Ratio

The concentration of aluminum hydroxide was fixed at 105 mmol (9.375g), and the reaction time and temperature were set at 3 h, 200°C, respectively. The amount of TIS was varied from 25, 50, 75, 100, to 125 mmol. The relationship between the mole ratio of TIS and % ceramic yield of the product, as shown in Figure 3.2 indicates that the curve is linear. When the mole ratio of TIS increases from 25 to 125 mmol, percent ceramic yield is significantly reduced. In this case, percent ceramic yields are in the range of 30-33 % which is higher than the theoretical ceramic yield (23.61 %). The higher % ceramic yield might result from the presence of smaller units of oligomers in the product. The reason might be that there is another side reaction competing with the intended reaction. For example, the condensation reaction of EG by TIS, as a catalyst, probably results in undesirable products. At very low concentration of TIS, EG is the major part of the reaction and TIS may act as catalyst to produce a product such as Al-EG [Petchsuk et al., (1995)] which gives a higher % ceramic yield than the expected product.

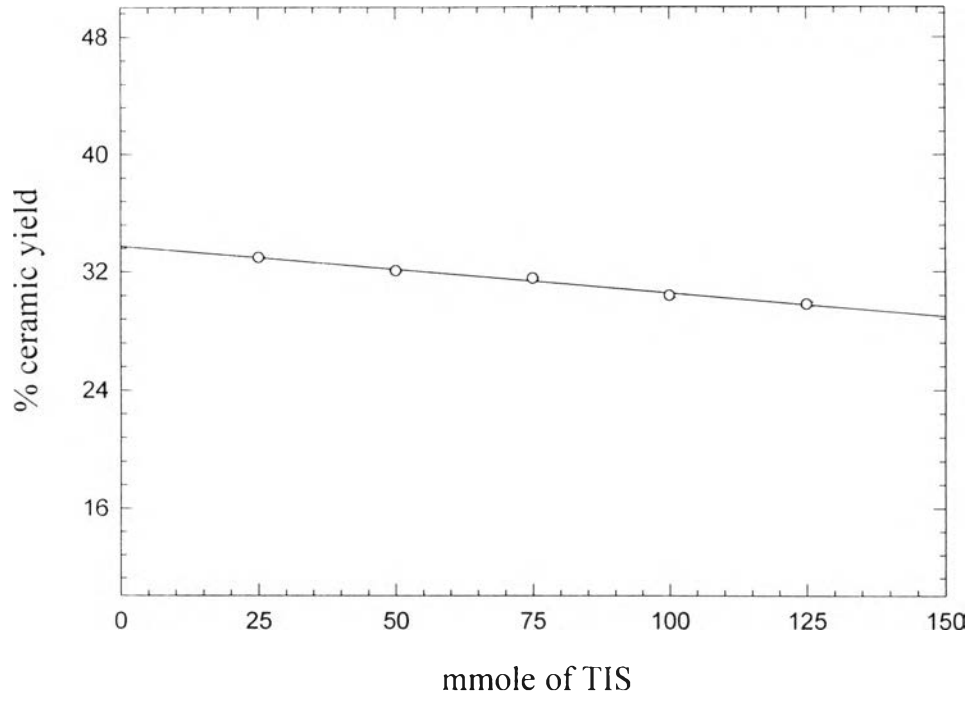

Figure 3.2 The relation between the mole ratio of TIS and % ceramic yield at the reaction time of 3 h and the reaction temperature 200°C (w/oTETA).

3.1.2 Reaction Time Variation

The amount of $Al(OH)_3$ and TIS were fixed at 9.375g (105mmol) and 9.6067g (50 mmol), respectively. The reaction time was varied from 60, 90, 120, 150, 180, to 240 minutes. The reaction temperature was controlled at 200±1°C. The relationship between the reaction time and % ceramic yield of the product is shown in Figure 3.3. At short reaction time (1-1.5 h.), percent ceramic yields are in the range of 39-40 %. As reaction time increases above 3 h of reaction time, the percent ceramic yield decrease to an

asymptote value of about 30 %, indicating that the reaction has gone to completion.

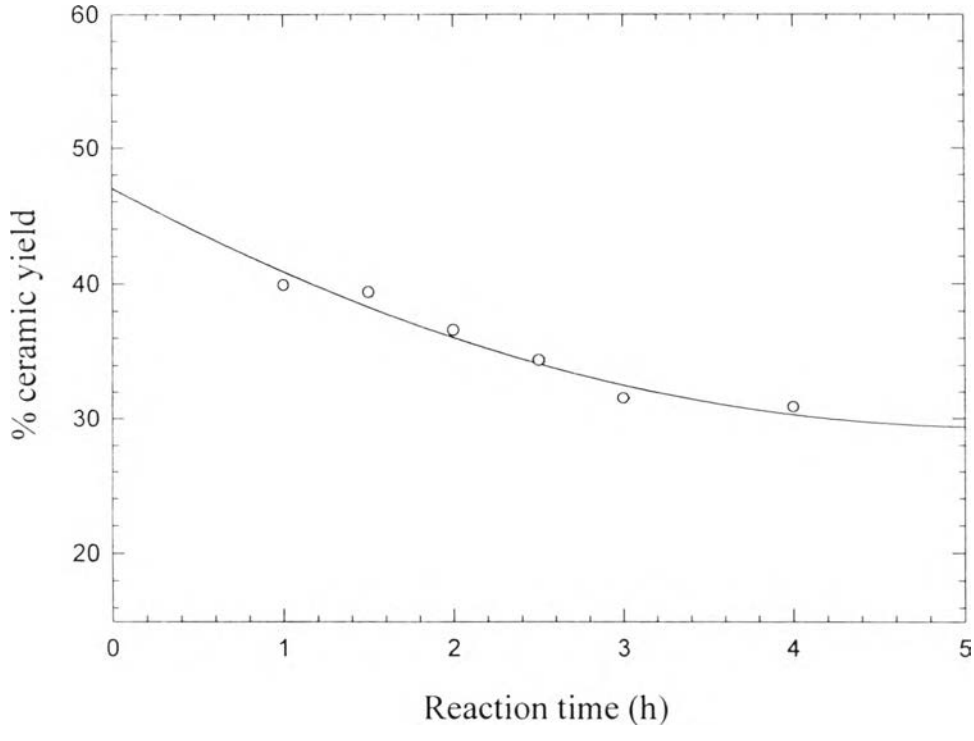

Figure 3.3 The relations between the reaction time and % ceramic yield at $Al(OH)_3$:TIS = 1:1 and the reaction temperature of 200°C (w/o TETA).

3.1.3 Reaction Temperature Variation

The experiments were carried out by fixing the amount of $Al(OH)_3$ and TIS at 9.375g (105 mmol) and 9.6067g (50 mmol), respectively. The reaction temperature was varied from 150°, 170°, 190°, 200°, 210°, to 220°C and the reaction time was set at 3 h. The relationship between the reaction temperature and % ceramic yield of the product, is illustrated in Figure 3.4. At lower reaction temperatures (150°-190°C), the percent ceramic

yield is dramatically increased from 30 to 46 %. Above 190°C to 220°C, percent ceramic yields are in the range of 32-29 %. As expected, higher reaction temperature gives lower % ceramic yields, meaning that more organic ligands relative to alumina are incorporated in the product.

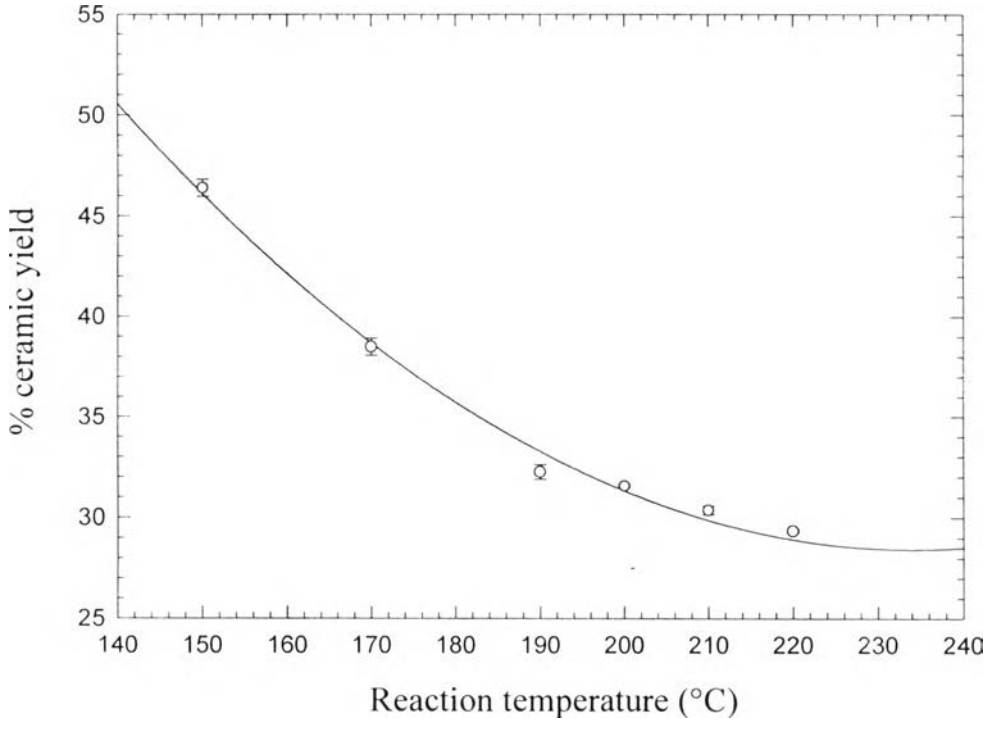

Figure 3.4 The relationship between the reaction temperature and % ceramic yield at $Al(OH)_3$: TIS = 1:1 and the reaction time of 3 h (w/oTETA).

3.1.4 Variation of TETA Concentration

The experiments were performed by fixing the amount of $Al(OH)_3$ and TIS at 9.375g (105 mmol) and 9.6067g (50 mmol), respectively. The reaction time and temperature were fixed at 3 h. and 200°C, respectively. The added mmol of catalyst, TETA, was varied from 25, 50, 75, 100, 125, to

150 mmol. The plot of the relationship between mole ratio of TETA and % ceramic yield is presented in figure 3.5. The curve shows a slight decrease in % ceramic yield when the TETA concentration is increased. The range of % ceramic yield is 26-30 % which is slightly lower than the reaction without TETA, suggesting that TETA catalyzes the reaction to allow more TIS to react with $Al(OH)_3$.

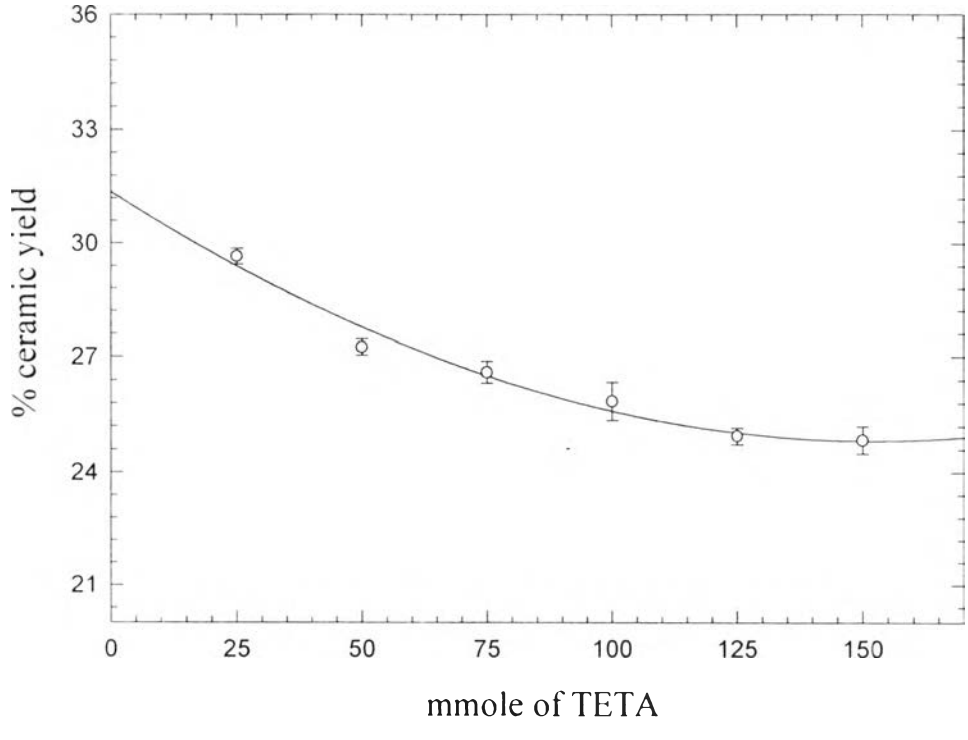

Figure 3.5 The relationship between the mole ratio of TETA and % ceramic yield at $Al(OH)_3$:TIS = 1:1, the reaction time of 3 h, and the reaction temperature of 200°C.

3.2 Characterization of Alumatrane Complexes

3.2.1 Thermogravimetric Analysis

The TGA profile for the product obtained from the reaction without TETA (Figure 3.6) shows two major regions of mass loss during heating. The first region is between 150°-250°C indicating the decomposition of TIS which is a component of the product . The second region occurs at about 250°-550°C, corresponding to the oxidative decomposition of the organic ligands and the carbon residues. The percent ceramic yield of the product is 32.1%.

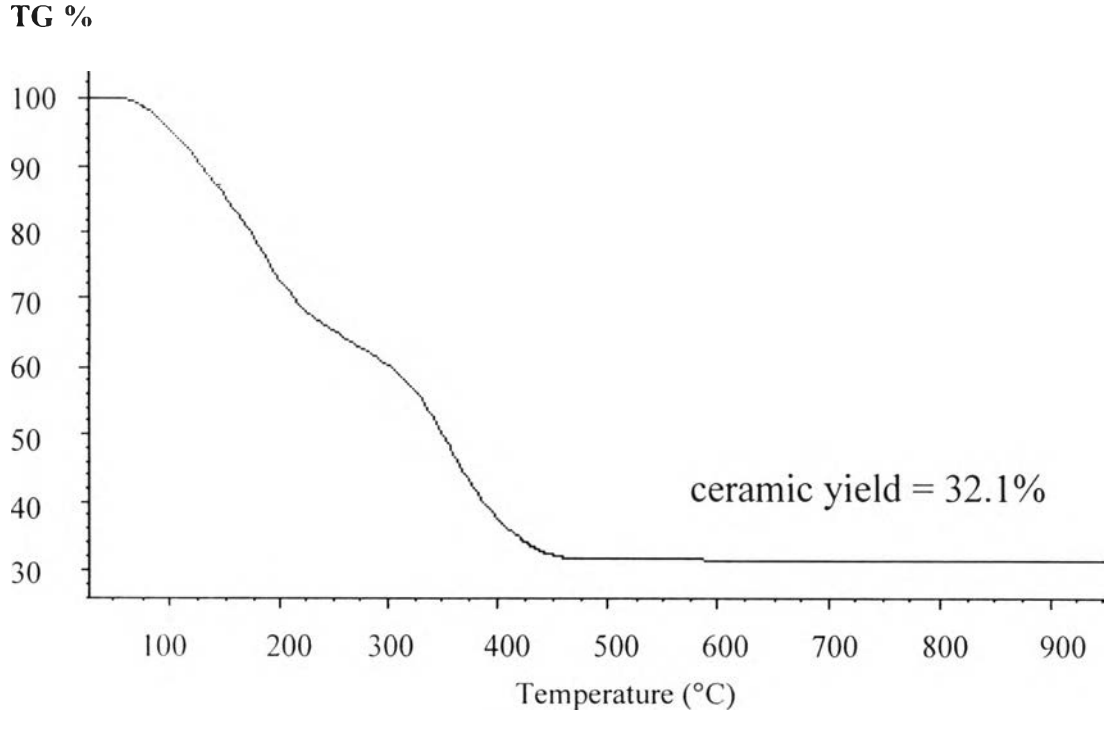

Figure 3.6 TGA Thermogram of the product obtained from the reaction without TETA.

The TGA of the product synthesized in the presence of TETA (Figure 3.7) shows two major mass losses. The first one at 160°-275°C corresponds to the oxidative decomposition of organic ligands. The second mass loss occurs at 275°-575°C indicating the oxidation of residual carbon. The percent ceramic yield of the product is 26.1%, lower than that of the product synthesized without TETA. In the presence of TETA, the product has a higher organic ligand to alumina ratio.

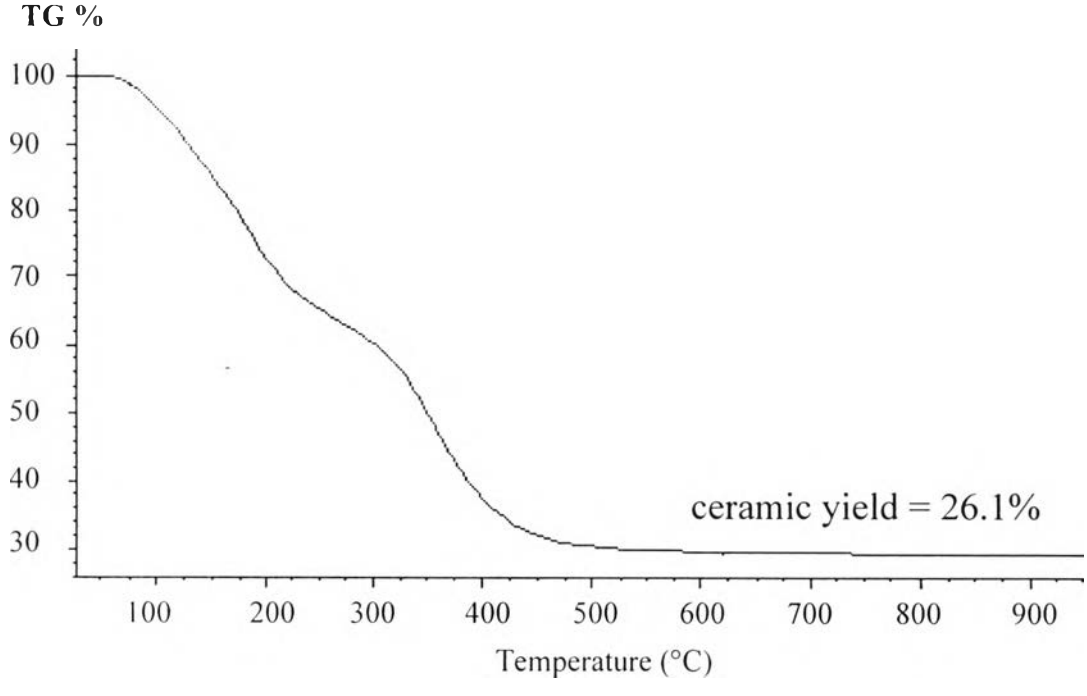

Figure 3.7 TGA Thermogram of the product from the reaction with TETA.

3.2.2 Fourier Transform Infrared Spectroscopy

The FTIR spectra of the products from the reaction with and without TETA are shown in Figure 3.8. Peak positions and assignments are listed in Table 3.1. Both spectra show similar functional groups. The broad peaks at 3000-3500 cm^{-1} correspond to ν O-H and ν C-H. The multiple peaks at 2750-3000 cm^{-1} represent the $-CH_2$ and $-CH_3$ stretches from TIS which is a component in the product. The singlet peak at about 1650 cm^{-1} is O-H overtone and C-H bending. The medium peak at 1375 cm^{-1} is $-CH_3$ bending from TIS. The strong peaks at 1000-1250 cm^{-1} result from the ν C-N and O-H bending. The broad peak at 500-800 cm^{-1} represents the ν Al-O of the product.

Table 3.1 Peak positions and assignments of FTIR spectra of the products with/ without TETA

Peak Positions		Assignments
Al-TIS	TIS-Al-TETA	
3000-3500	3000-3500	ν O-H and ν C-H
2750-3000	2750-3000	ν C-H
1650	1630	O-H overtone; C-H bending
1460	1450	δ C-H
1375	1375	δ C-H
1000-1250	1000-1200	ν C-N; O-H bending
500-850	500-800	ν Al-O

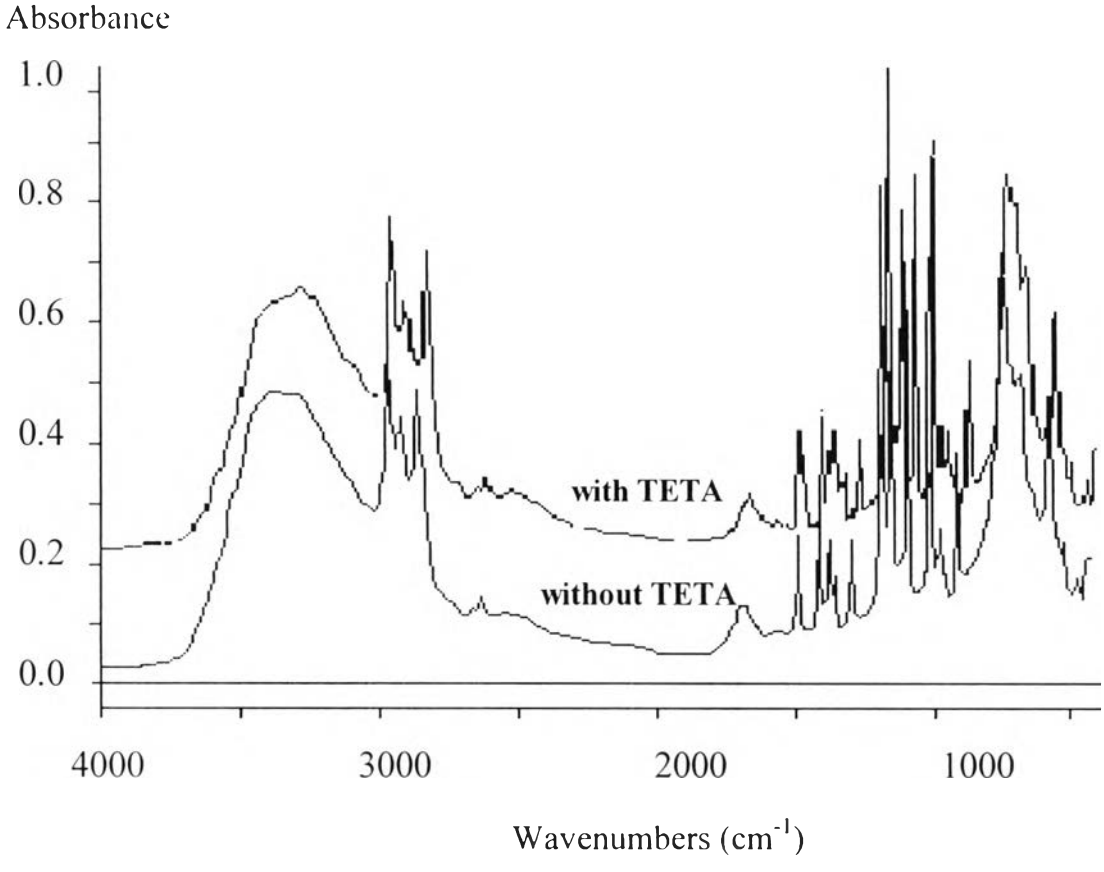

Figure 3.8 FTIR spectra of the products from the reactions with and without TETA.

3.2.3 Nuclear Magnetic Resonance Spectroscopy

The NMR spectra of the products from the reactions with and without TETA are shown in Figures 3.9-3.10, respectively. Peak positions and assignments are listed in Table 3.2.

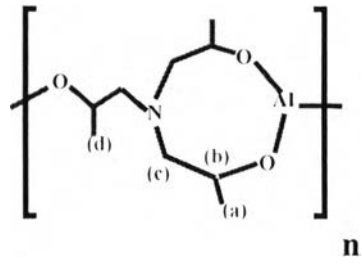

Figure 3.9 The proposed model from NMR spectra of the products.

The ^{1}H-NMR spectrum of the product from the reaction without TETA shows 6 groups of peak. The doublet peaks at 1.07-1.11 ppm correspond to the -CH_3 group of TIS (position (a)). The overlap doublet peaks at 1.10-1.13 ppm are assigned to the -CH_3 group of TIS (position (d)) which occurring on the arm that connect to hydroxyl group (end chain). The multiplet peaks at 2.29-2.90 ppm are assigned to the methylene group adjacent to the N-atom of TIS (-N-CH_2) at position (c). The multiplet peaks at 3.82-4.23 ppm are assigned to the tertiary carbon adjacent to the O-atom of TIS, position (b). The sharp peaks at 3.28-3.32 ppm come from the methyl group of the methanol solvent. The singlet peak at 4.70-4.98 ppm represents the water absorption in the solvent and is assigned to the proton of Al-OH occurring at the end chain. The ^{1}H-NMR spectrum of the product from the reaction with TETA gives a similar spectrum.

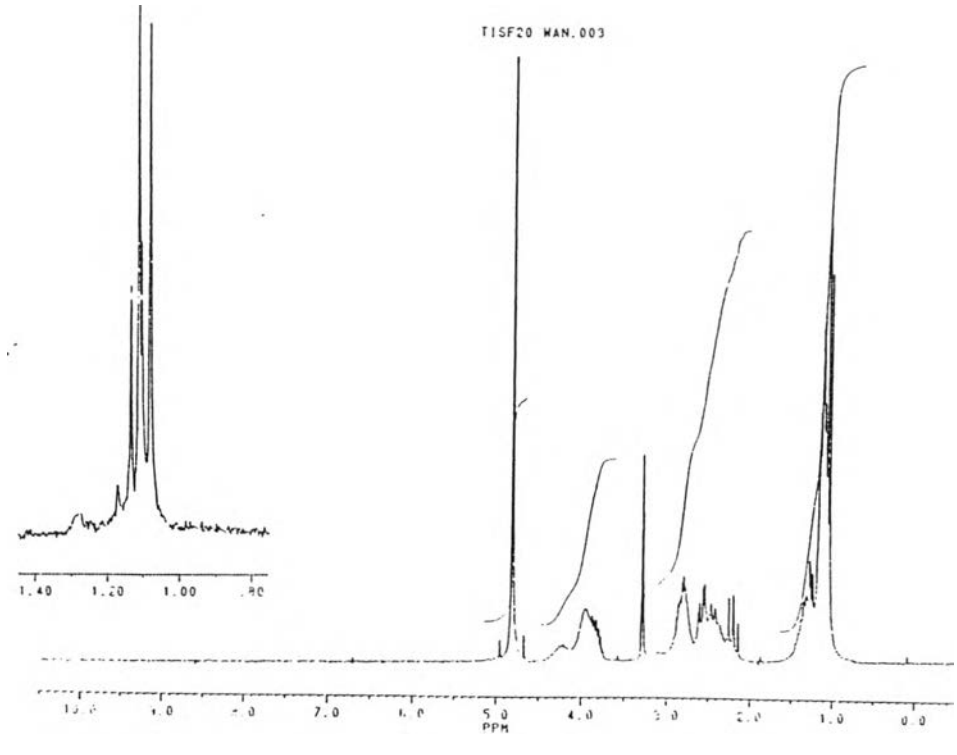

Figure 3.10 ^{1}H-NMR spectrum of the product without TETA.

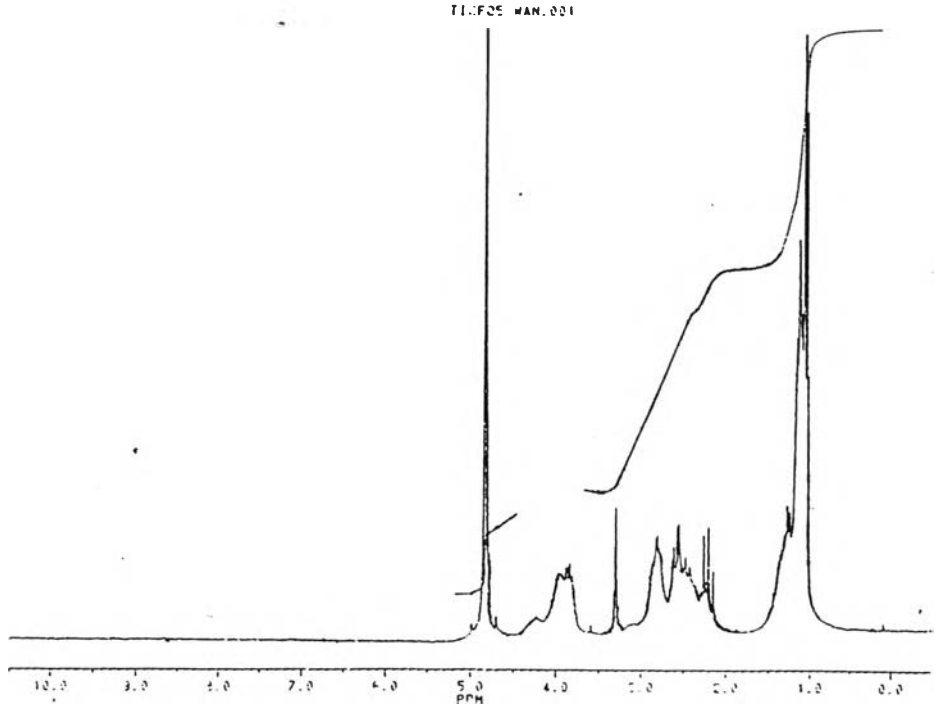

Figure 3.11 ^{1}H-NMR spectrum of the product with TETA.

Table 3.2 Peak positions of ^{1}H-NMR of products

Compounds	^{1}H-NMR (ppm)
Product w/o TETA	1.01-1.11(a) 1.10-1.13(d) 2.29-2.90(c) 3.82-4.23(b)
Product w/ TETA	1.06-1.11(a) 1.12-1.15(d) 2.32-2.63(c) 3.78-4.23(b)

3.3 Viscosity Measurement

In this section, the viscous properties of the synthesized products in solution were determined using a capillary viscometer.

3.3.1 Effect of TIS Concentration

Figure 3.12 shows the reduced specific viscosity plotted versus polymer concentration as a function of TIS concentration. The measurements were taken at 30°C. The reduced viscosity of the polymer solutions increases linearly with TIS concentration.

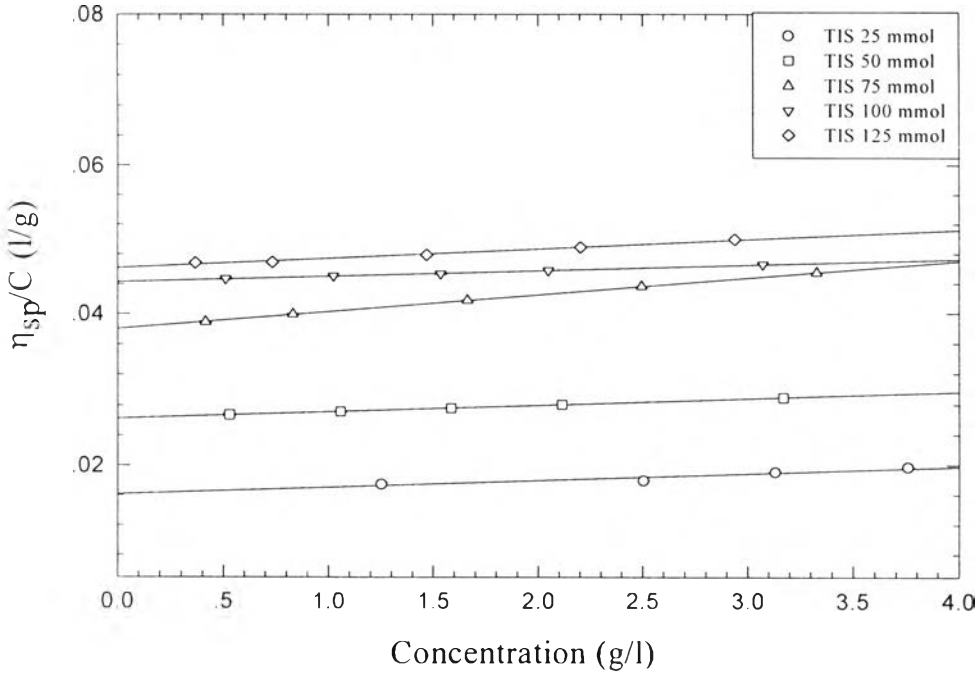

Figure 3.12 Reduced specific viscosity versus polymer concentration as a function of TIS concentration at the reaction temperature of 200°C and the reaction time of 3 h (without TETA).

Figure 3.13 shows the inherent viscosity plotted as a function of polymer concentration in terms of TIS concentration. The inherent viscosity also increases linearly with TIS concentration.

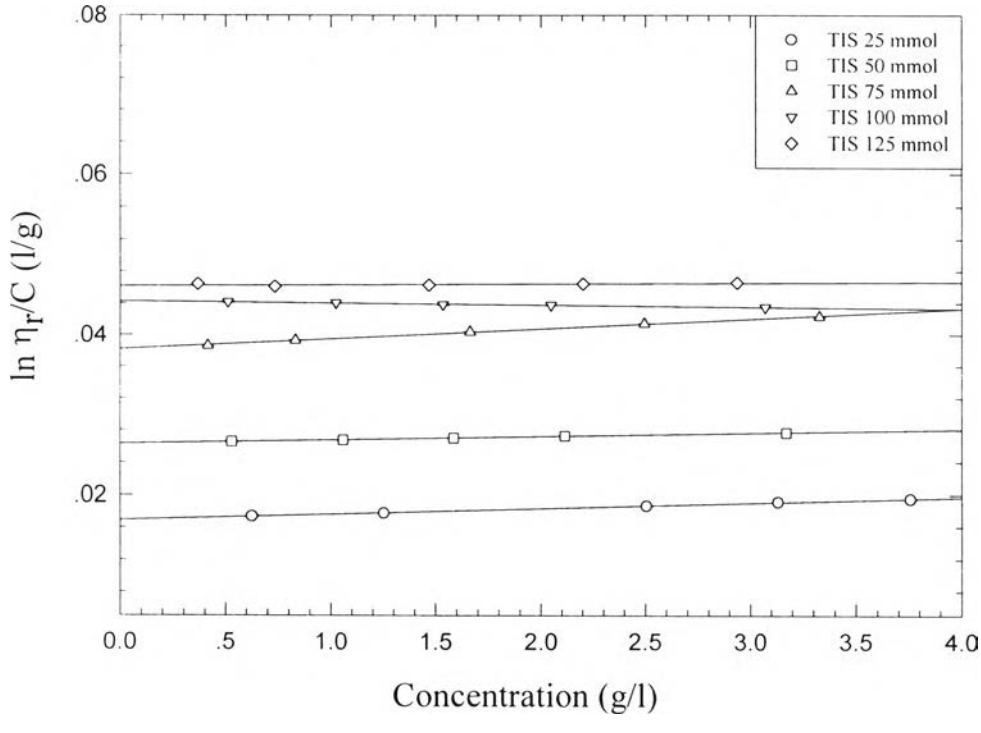

Figure 3.13 Inherent viscosity of the polymer solution as a function of TIS concentration at the reaction temperature of 200°C and the reaction time of 3 h (without TETA).

Figure 3.14 shows the intrinsic viscosity plotted versus polymer concentration as a function of TIS concentration. The intrinsic viscosity was calculated from Figure 3.12 via the Huggins equation (eq.2.7), and from Figure 3.13 via the Kraemer equation (eq.2.8). When the mole ratio of TIS increases from 25 to 100 mmol, the intrinsic viscosity increases from 0.02 to 0.05 g/l. The intrinsic viscosity does not change when the TIS concentration is

greater than 125 mmol. Therefore the optimum ratio to synthesize the longest chain is 125 mmol of TIS for 100 mmol of $Al(OH)_3$.

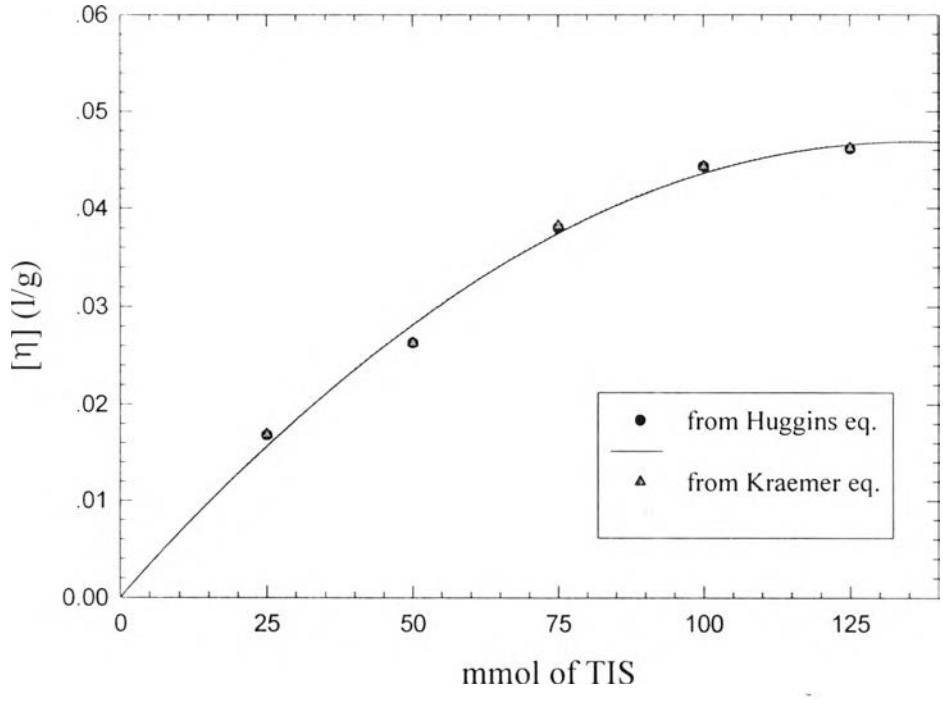

Figure 3.14 Comparing the intrinsic viscosity from Huggins eq. (●) and Kraemer eq.(▲) as a function of TIS concentration by fixed the condition at $Al(OH)_3$ =100 mmol, the reaction temperature of 200°C and the reaction time of 3 h (without TETA).

The parameters k' and k'' from, respectively, the Huggins and Kraemer equations can give us the information about the polymer-solvent interaction. The parameter k' assumes a value between 0.4-0.8 for generally good solvent and above 0.8 for a theta solvent [G.B Howard and W.M. Jimmy, (1991)]. The values of the intrinsic viscosites, k', k'', and the overlap concentration are shown in Table 3.3.

Table 3.3 Viscometric properties of alumatrane complexes in dilute solution as a function of TIS concentration at $Al(OH)_3$ = 100 mmol, the reaction temperature of 200°C and the reaction time of 3 h (without TETA)

mmol of TIS	[η]* (l/g)	[η]** (l/g)	K'	k''	C* (g/l)
25	0.017	0.017	3.2	-2.42	60
50	0.026	0.026	1.2	-0.64	38
75	0.038	0.038	1.6	-0.88	26
100	0.044	0.044	0.4	+0.12	23
125	0.046	0.046	0.6	-0.11	28

* for the Huggins equation

** for the Kraemer equation

From Table 3.3, the data suggests that the intrinsic viscosities from both equations are nearly the same. The Huggins parameter (k') shows that, at lower TIS concentration (25-75 mmol), ethylene glycol is not a good solvent for our polymer system whereas at higher concentration of TIS, especially at 100 mmol, polymer can dissolve better due to the higher polymer-solvent interaction. The values of k' and k'' are in good agreement with the theoretical relation $k' + k'' = 1/2$. The overlap concentration, C*, can give us the approximately overlap concentration between dilute and semidilute regimes. As can be seen in this table, the overlap concentrations of polymer solutions are in the range of 21-60 g/l, therefore our products were studied in the dilute regime.

3.3.2 Effect of Reaction Time

The relation between the reduced specific viscosity of the polymer solutions and reaction time are shown in Figure 3.15. η_{sp}/c increases linearly with polymer concentration.

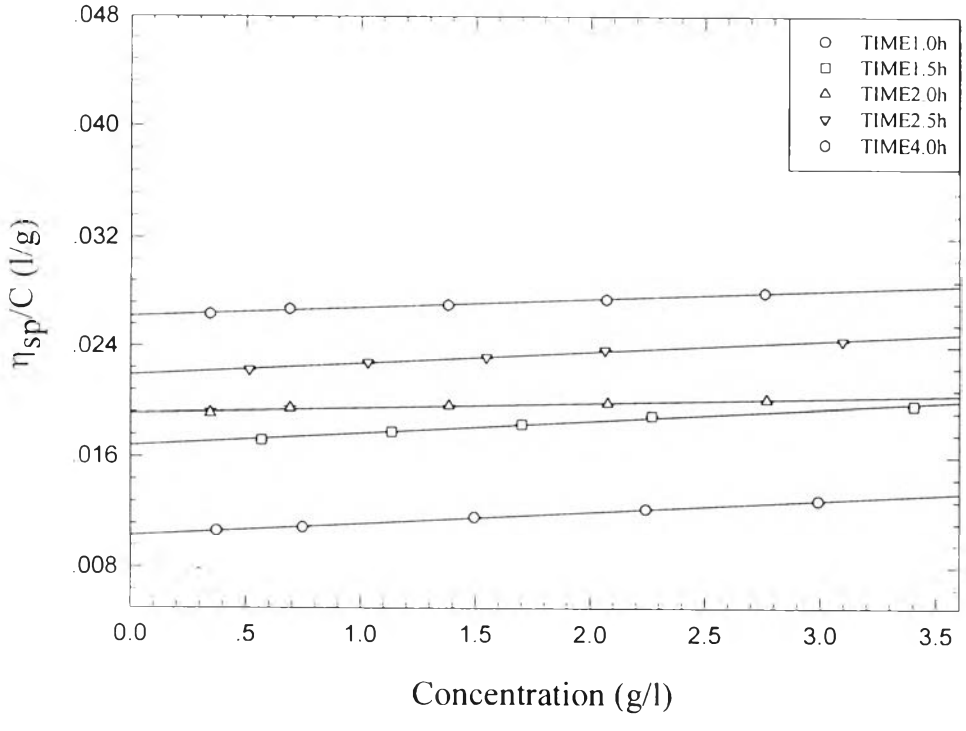

Figure 3.15 Reduced specific viscosity versus polymer concentration as a function of reaction time at $Al(OH)_3$:TIS = 1:1 and the reaction temperature of 200°C (without TETA).

Figure 3.16 shows the inherent viscosity plotted versus polymer concentration as a function of reaction time. The inherent viscosity increases linearly with polymer concentration.

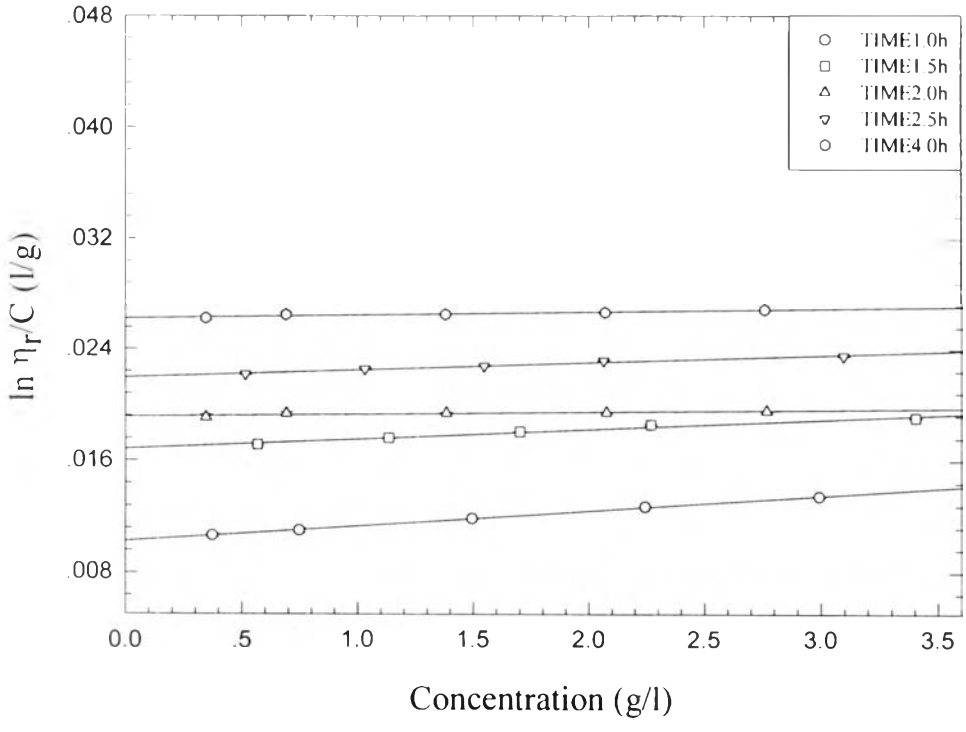

Figure 3.16 Inherent viscosity of the polymer solution as a function of reaction time at $Al(OH)_3$:TIS = 1:1 and the reaction temperature of 200°C (without TETA).

As shown in Figure 3.17, the intrinsic viscosity of the polymer solutions increases with reaction time. After 4 h of reaction time, the intrinsic viscosity approaches a constant value, meaning that the reaction is complete and perhaps that highest molecular weight chains would be obtained from the reaction.

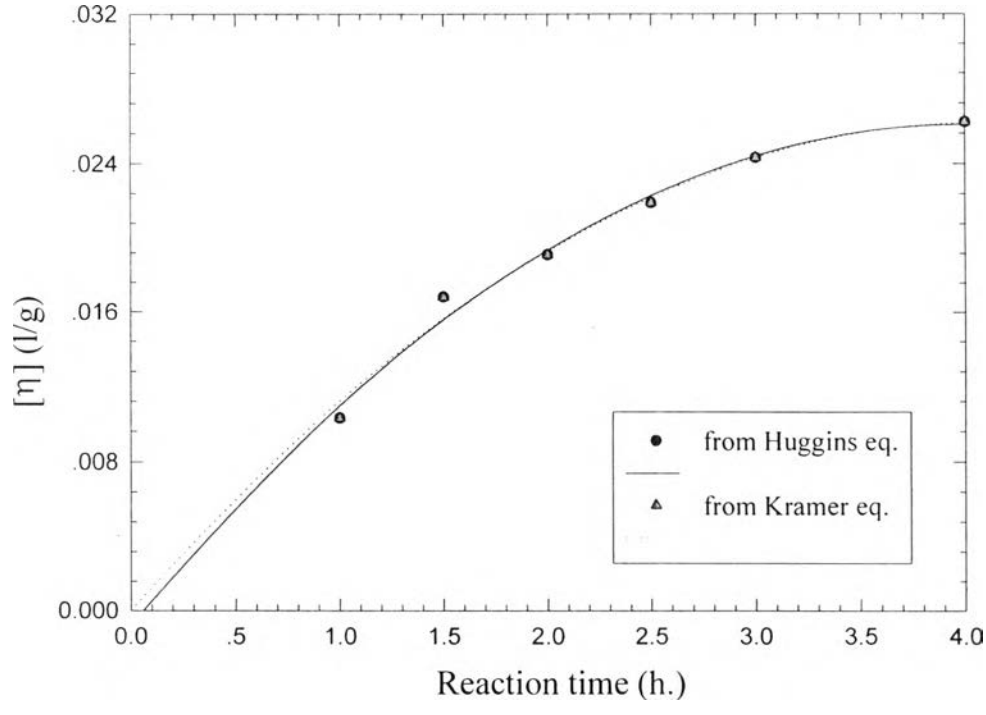

Figure 3.17 Comparing the intrinsic viscosity from Huggins eq. (●) and Kraemer eq.(▲) as a function of the reaction time at $Al(OH)_3$:TIS = 1:1 and the reaction temperature of 200°C (without TETA).

Table 3.4 shows the list of intrinsic viscosities from Huggins ([η]*) and Kraemer equations ([η]**), the parameters k' and k'', and the overlap concentration as a function of reaction time.

Table 3.4 Viscometric properties of alumatrane complexes in dilute solution as a function of reaction time at $Al(OH)_3$:TIS = 1:1 and the reaction of temperature 200°C (without TETA)

Reaction time (h)	[η]* (l/g)	[η]** (l/g)	k'	k''	C* (g/l)
1.0	0.010	0.010	7.8	-7.3	97
1.5	0.017	0.017	3.7	-3.0	60
2.0	0.019	0.019	3.6	-2.9	52
2.5	0.022	0.022	1.8	-1.1	46
4.0	0.026	0.026	0.9	-0.4	38

* for the Huggins equation

** for the Kraemer equation

According to the table, the intrinsic viscosities calculated from both equations are nearly the same. At shorter reaction time, the reaction may be incomplete; as a result, short chains occur as a major product. Therefore, the intrinsic viscosity of the product at the shorter reaction time is lowest. Furthermore, the values of the parameters k' and k'', show that the solvent is poor; in comparison to the products at short reaction time, the polymer dissolves better when longer reaction time is used.

3.3.3 Effect of Reaction Temperature

The relationships between the reduced specific viscosity of the polymer solutions and the reaction temperatures are shown in Figure 3.18. The polymer - solvent interaction would appear to be similar for different reaction temperatures. The linearity of the reduced specific viscosity plot confirms that the polymer solutions were studied in the dilute regime.

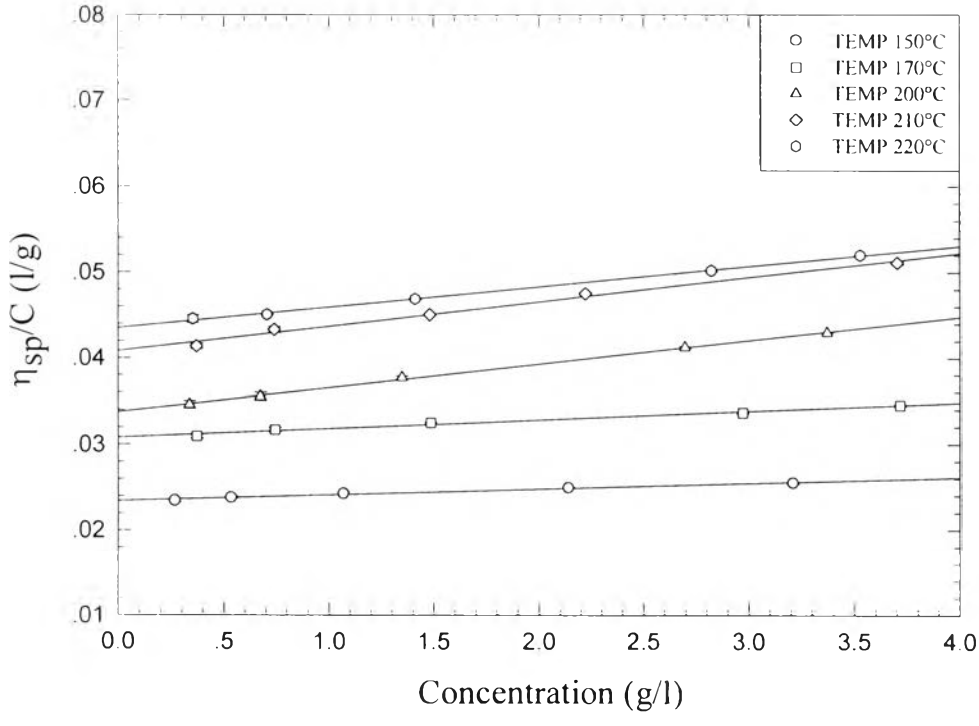

Figure 3.18 Reduced specific viscosity versus polymer concentration as a function of reaction temperature at $Al(OH)_3$:TIS = 1:1 and the reaction time of 3 h (without TETA).

Figure 3.19 shows the inherent viscosity plotted versus polymer concentration as a function of reaction temperature. The inherent viscosities of the polymer solution increase linearly with the reaction temperature.

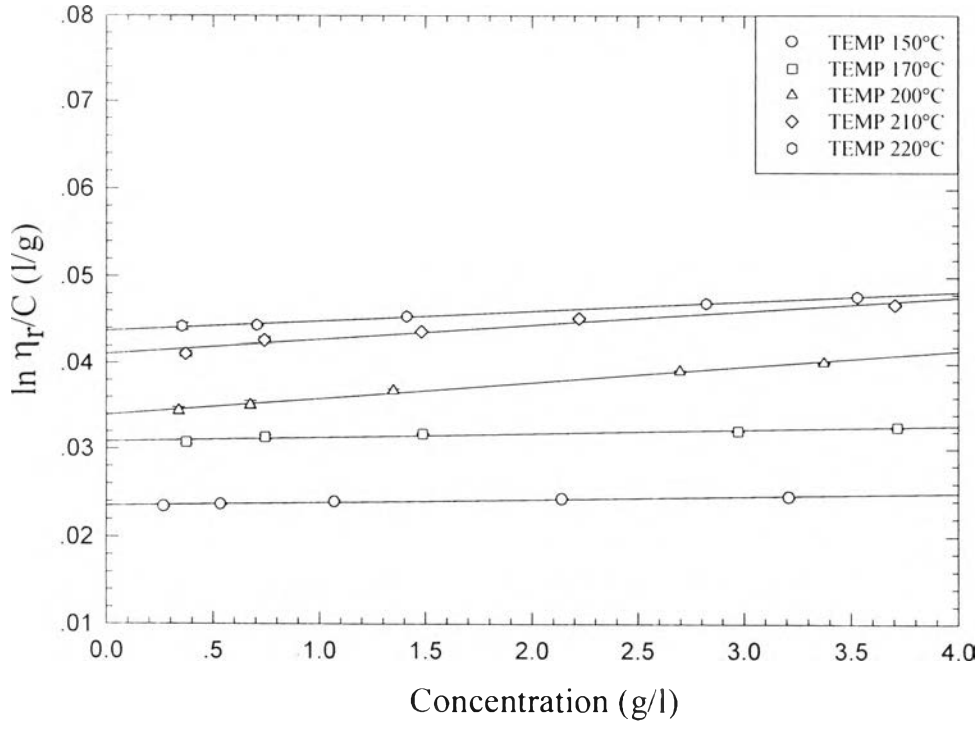

Figure 3.19 Inherent viscosity versus polymer concentration as a function of the reaction temperature at $Al(OH)_3$:TIS = 1:1 and the reaction time of 3 h (without TETA).

Figure 3.20 shows the intrinsic viscosity of the polymer solutions plotted as a function of reaction temperature. This figure shows that at a higher reaction temperature, a higher intrinsic viscosity of the polymer solutions is obtained. In fact, at a higher reaction temperature, the reaction is faster due to the fact that the byproducts, ethylene glycol and water, are distilled off. The disadvantage for using high temperature is the difficulty in controlling the reaction; a high temperature reaction causes undesirable decomposition of the product.

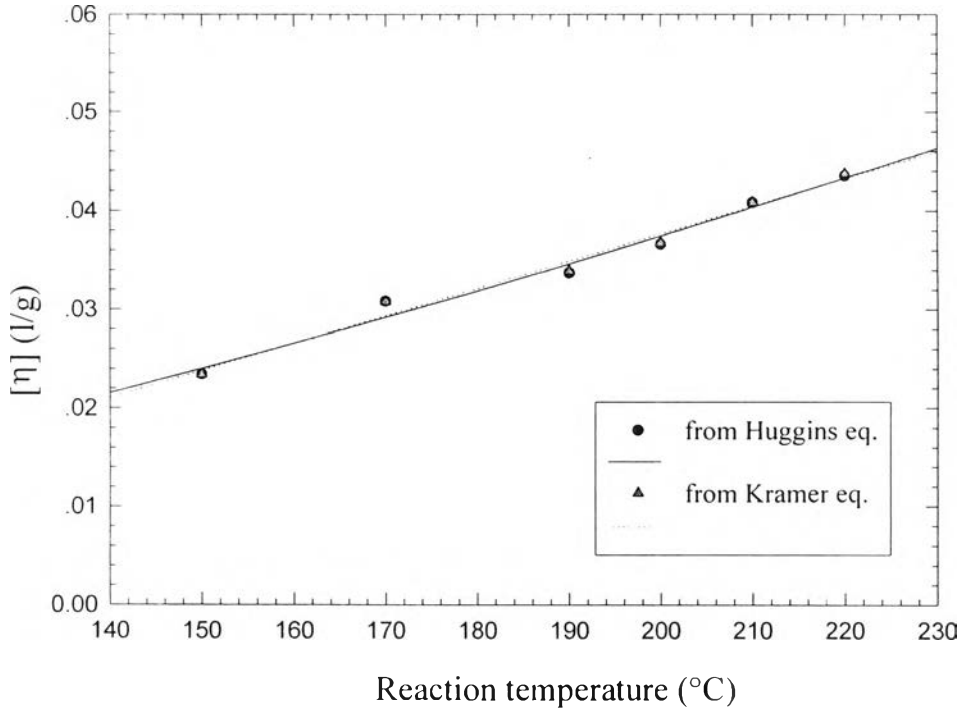

Figure 3.20 Comparing the intrinsic viscosity from Huggins eq. (●) and Kraemer eq.(▲) as a function of the reaction temperature at $Al(OH)_3$:TIS = 1:1and the reaction time of 3 h (without TETA).

Table 3.5 lists the values of the intrinsic viscosities from both equations, the parameters k' and k'', and the overlap concentration. The Huggins parameters (k') are higher than 0.8, meaning that, ethylene glycol is a poor solvent for our polymer system. The overlap concentrations are in the range of 22-43 g/l.

Table 3.5 Viscometric properties of alumatrane complexes in dilute solution as a function of the reaction temperature at $Al(OH)_3$:TIS = 1:1 and the reaction time of 3 h (without TETA).

Reaction temperature (°C)	[η]* (l/g)	[η]** (l/g)	k'	k''	C* (g/l)
150	0.023	0.023	1.2	0.55	43
170	0.031	0.031	1.2	0.57	33
200	0.037	0.037	1.1	0.41	27
210	0.041	0.041	1.4	0.84	25
220	0.044	0.044	1.3	0.60	23

* for the Huggins equation

** for the Kraemer equation

3.3.4 Effect of TETA concentration

The reduced specific viscosities as a function of the amount of catalyst, TETA, are plotted in Figure 3.21. It was found that the reduced viscosity of the polymer solution increases linearly with polymer concentration. The interaction between different polymers and the solvent are also quite different.

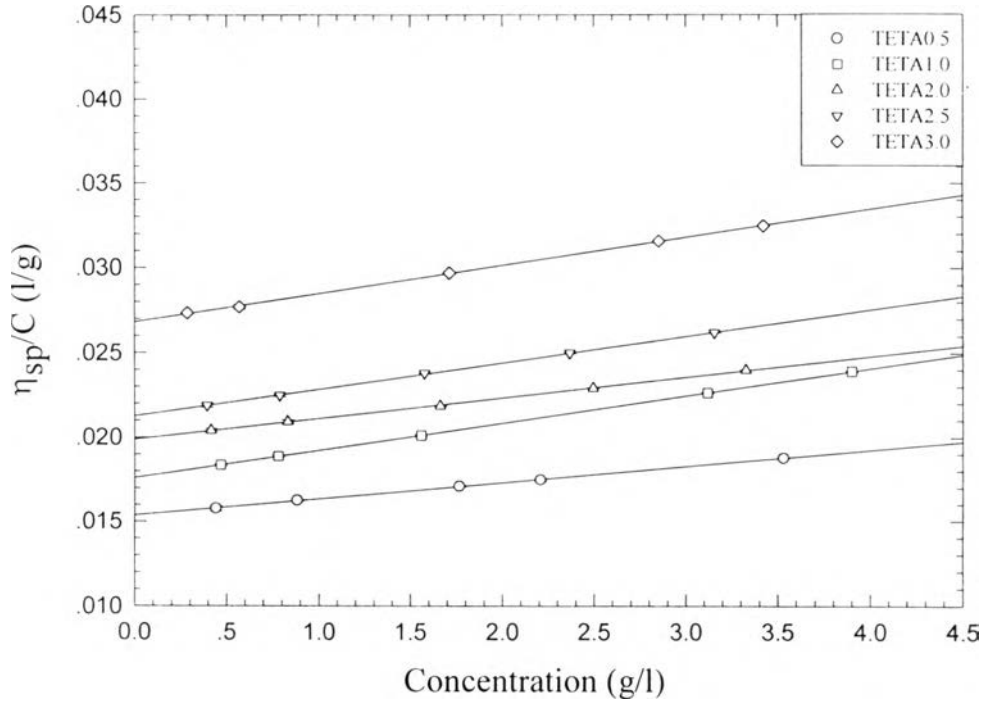

Figure 3.21 Reduced specific viscosity versus polymer concentration as a function of TETA concentration at $Al(OH)_3$:TIS = 1:1, the reaction time of 3 h, and the reaction temperature of 200°C.

Figure 3.22 shows the inherent viscosity plotted as a function of TETA concentration. The inherent viscosity increases linearly with polymer concentration.

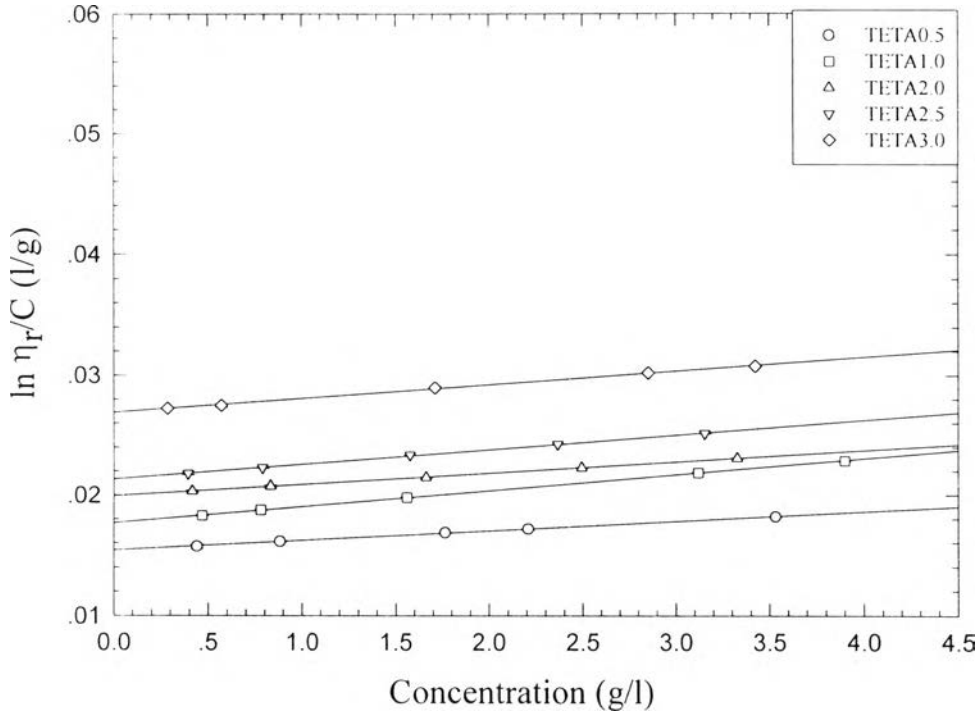

Figure 3.22 Inherent viscosity versus polymer concentration as a function of TETA concentration at $Al(OH)_3$: TIS = 1:1, the reaction time of 3 h, the reaction temperature of 200°C.

Figure 3.23 shows the intrinsic viscosity as a function of catalyst concentration. The intrinsic viscosity increases with the amount of catalyst. The value of intrinsic viscosities, parameters k' and k'', and the overlap concentration are listed in Table 3.6.

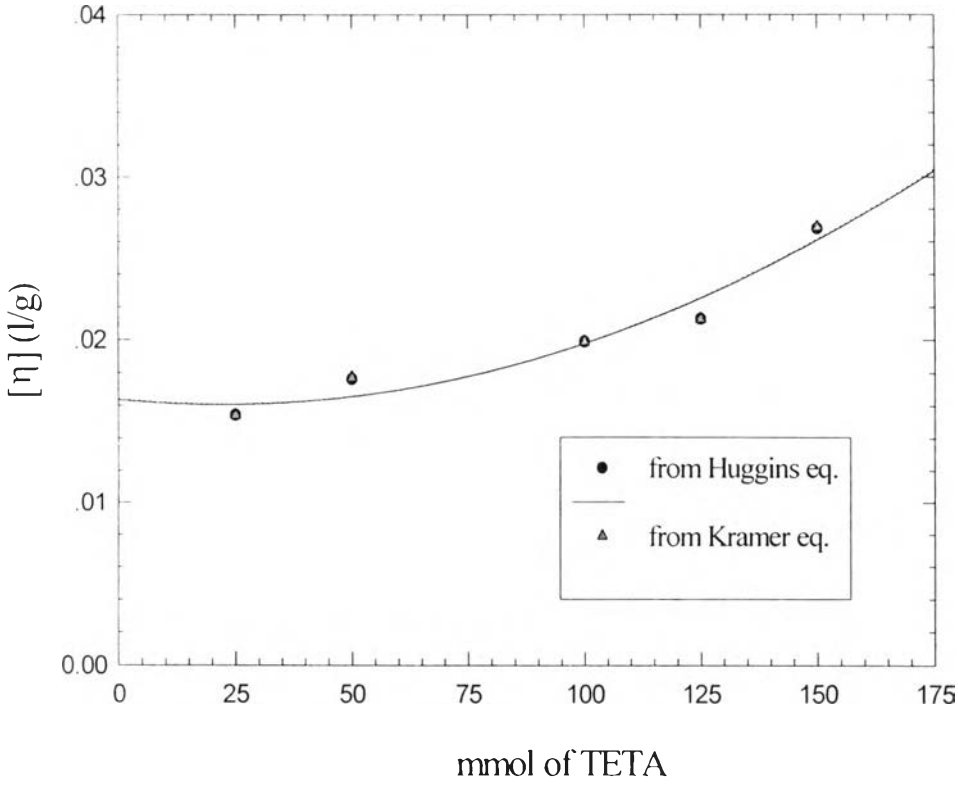

Figure 3.23 Comparing the intrinsic viscosity from Huggins eq. (●) and Kraemer eq. (▲) as a function of TETA concentration at $Al(OH)_3$: TIS = 1:1, the reaction time of 3 h, and the reaction temperature of 200°C.

Table 3.6 Viscometric properties of alumatrane complexes in dilute solution as a function of catalyst, TETA, concentration at $Al(OH)_3$: TIS = 1:1, the reaction time of 3 h, and the reaction temperature of 200°C

mmol of TETA	[η]* (l/g)	[η]** (l/g)	k'	k''	C* (g/l)
0	0.015	0.015	5.1	-4.5	65
25	0.015	0.015	4.1	-3.4	65
50	0.018	0.018	5.2	-4.3	57
75	0.019	0.019	4.0	-3.4	55
100	0.020	0.020	3.1	-2.4	50
125	0.021	0.021	3.5	-2.7	47
150	0.027	0.027	2.3	-1.6	37

* for the Huggins equation

** for the Kraemer equation

The intrinsic viscosity from the reaction with TETA is higher than that from the reaction without TETA. Therefore, at the same condition, TETA can catalyze the reaction to give a greater interaction between TIS and $Al(OH)_3$ or to produce higher molecular weight polymers. From the Huggins parameter, we can conclude that the ethylene glycol is a poor solvent for the polymer and the polymer-solvent interaction trends to increase when a higher amount of TETA was used.

3.4 Dynamic Light Scattering (DLS)

In this section, dynamic light scattering was used to investigate the hydrodynamic radius of the polymer as a function of TETA concentration. The analysis was carried out by plotting D_{app} vs the square of the scattering vector (q^2), and extrapolating the data to q^2=0 to get the center of mass diffusion, D_{cm}. The relation between the D_{app} and the q^2 is shown in Figure 3.24.

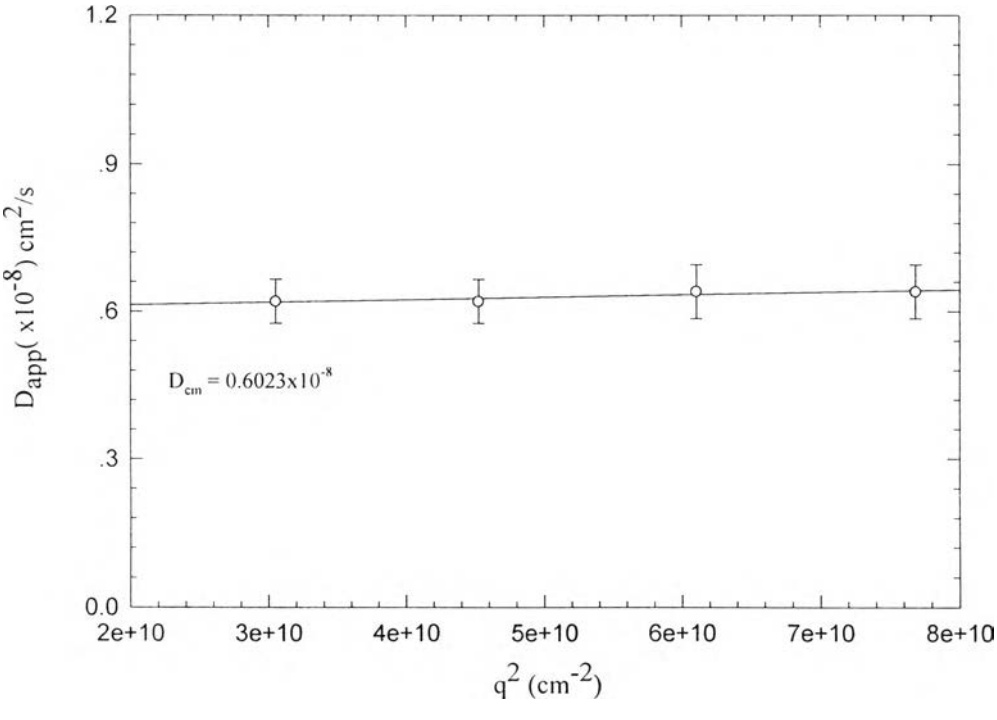

Figure 3.24 The relation between the apparent diffusion coefficient, D_{app}, and q^2 of the product synthesized using $Al(OH)_3$:TIS:TETA = 100 : 100 : 50 mmol, at the reaction time of 3 h, and the reaction temperature of 200°C.

In Figure 3.24, the center of mass diffusion, D_{cm} can be found from the intercept of the curve. In order to remove the effects of interparticle interactions on our experimental measurements, the diffusion coefficient, D_{cm}, can be extrapolated to zero concentration from the plot between D_{cm} and polymer concentration, as shown in Figure 3.25.

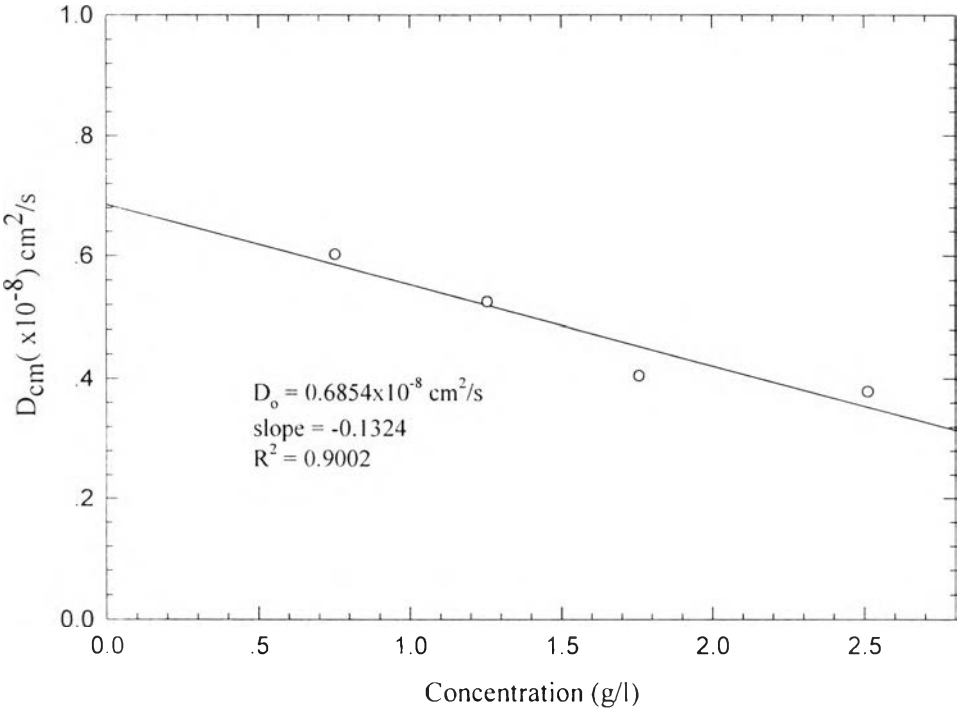

Figure 3.25 The center of mass diffusion coefficient (D_{cm}) as a function of polymer concentration of the product synthesized using $Al(OH)_3$:TIS:TETA = 100:100:50 mmol, at the reaction time of 3 h, and the reaction temperature of 200°C.

In the dilute-solution regime with ethylene glycol as a solvent, the concentration dependence of D_{cm} is linear. The small slope in Figure 3.25 indicates that concentration dependence is small [A.W.De Groot and D.E. Guinnup, (1991)]. This trend indicates little interaction between polymer

chains over this concentration range consistent with the deduction for the Huggins coefficient that the solvent is a poor one. Calculations of the infinite dilution diffusion coefficients, D_o, were carried out using a linear least squares on the data in Figure 3.25 to obtain the slope and intercept from the equation:

$$D_{cm} = D_o (1 + k_D c_p + ...), \qquad (3.1)$$

where D_o is the mutual diffusion coefficient at infinite dilution and D_{cm} is the value at concentration c_p. The parameter k_D is greater than the 0 for general good solvent and k_D is less than 0 for poor solvent [E.D., Goddard, (1993)]. From this figure, k_D is equal to -0.1324. Other R_H and k_D values are tabulated in Table 3.7. It can be seen that ethylene glycol is a poor solvent for this system, consistent with the viscosity results.

Table 3.7 The hydrodynamic radius and parameter k_D as a function of TETA concentration

mmol of TETA	R_H (nm)	k_D
0	18.60	-0.1247
50	19.04	-0.1324
75	19.89	-0.2347
100	20.64	-0.2688
125	22.91	-0.1858
150	24.18	-0.1553

Figure 3.26 shows the relation between the mutual diffusion coefficient, D_o, and the amount of TETA.

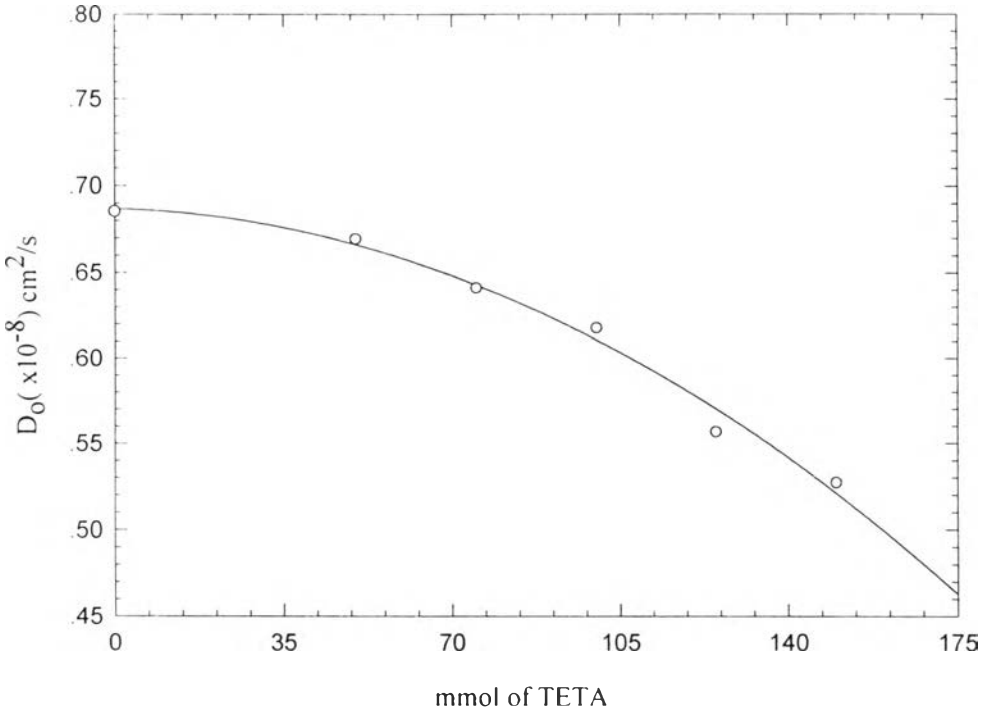

Figure 3.26 Diffusion coefficient as a function of TETA concentration of the product synthesized using $Al(OH)_3$:TIS:TETA = 100:100:50 mmol, the reaction time of 3 h, and the reaction temperature of 200°C.

The diffusion coefficient contains information about the size and the structure of particles in solution. From this figure, we found that the diffusion coefficient decreases with TETA content. The hydrodynamic radius, R_H, was obtained from D_o via the Stokes-Einstein (Eq. 2.17), the relation between hydrodynamic radius and the TETA concentration is plotted, and shown in Figure 3.27.

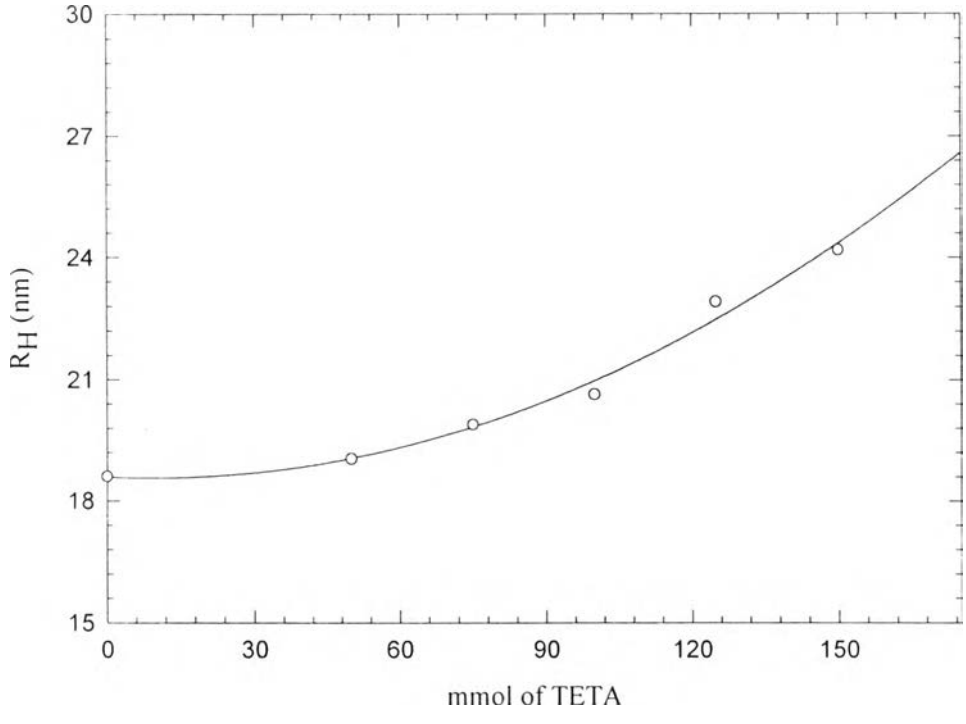

Figure 3.27 Hydrodynamic radius as a function of TETA concentration of the product synthesized using $Al(OH)_3$:TIS:TETA = 100:100:50 mmol, at the reaction time of 3 h, and the reaction temperature of 200°C.

The hydrodynamic radius is effectively the diameter of the volume occupied by the light scattering polymer as it moves about with kinetic energy. It may contain information about both the physical size of the polymer chains and the range of solution interactions which control the particle motion through frictional forces [Barth H.G., (1991)].

As can be seen from Figure 3.27, the hydrodynamic radius increases with increasing mmol of TETA. The increase of hydrodynamic radius can be correlated with the increase of the intrinsic viscosity of the polymer solution, as shown in Figure 3.28.

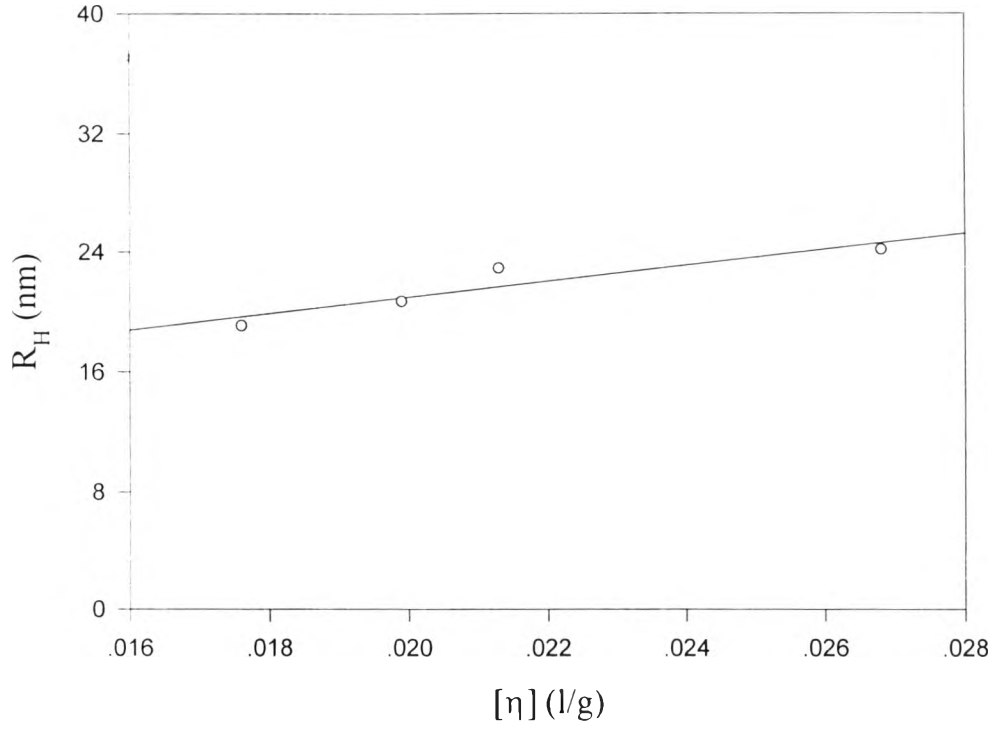

Figure 3.28 The relation between the hydrodynamic radius and the intrinsic viscosity as a function of catalyst concentration, the first point refers to TETA 50 mmol followed by 100, 125, and 150 mmol, respectively.

Figure 3.28 shows that the relation between the hydrodynamic radius and the intrinsic viscosity of the polymer solution is linear. Thus we can conclude that, in the present of TETA, the polymer has more interaction with the solvent as evidenced by the values of k′, k″, and k_D and the increases size of the polymer chains increases.

Figure 3.29 shows the polydispersity of the dynamic light scattering relaxation time for the product with TETA concentration of 50 and 150 mmol at 60° as a function of polymer concentration at 30°C.

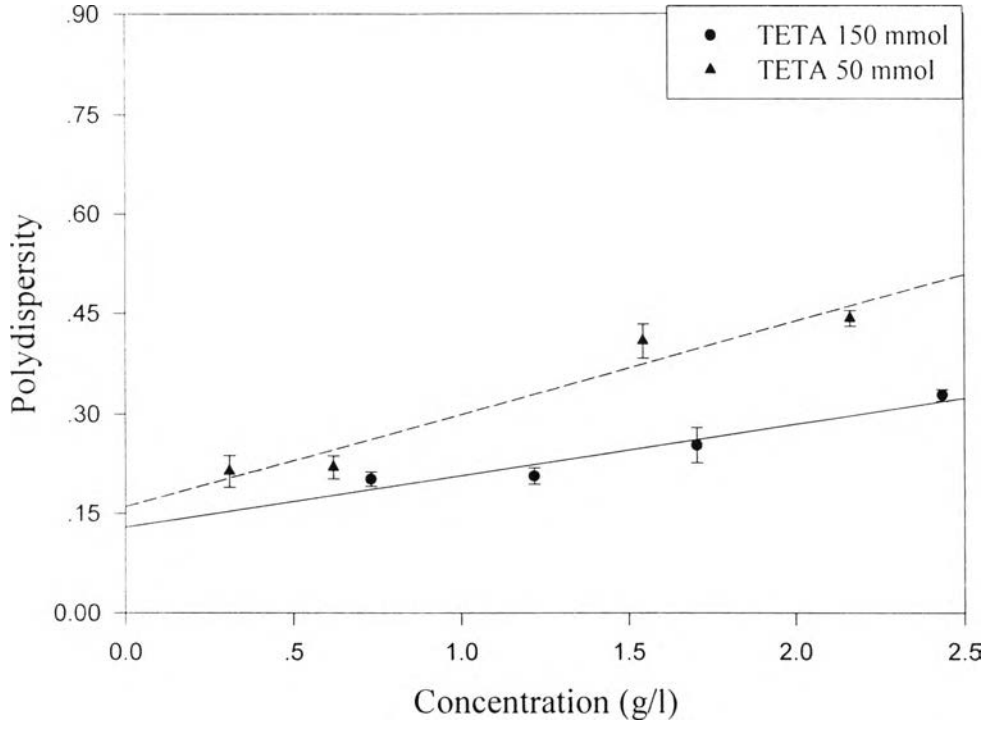

Figure 3.29 Polydispersity of relaxation time for the product with TETA 150 mmol (●) and 50 mmol (▲) solution at 60° as a function of polymer concentration at 30°C.

From this figure, the polydispersity of both TETA concentrations has the same trend; that is the polydispersity slightly increases with polymer concentration. The polydispersity of the polymer with TETA 50 mmol is higher than that of the polymer with 150 mmol, meaning that at low TETA content, the product consists of many sizes of polymer unit more than that from higher amount of TETA. The range of polydispersity covers from 0.16 to 0.30 for 150 mmol TETA, comparison to 0.15 to 0.40 for 50 mmol TETA.